Image Quality Analysis for Visible Spectral Imaging Systems

Qun Sun▲* and Mark D. Fairchild▲

Munsell Color Science Laboratory, Chester F. Carlson Center for Imaging Science, Rochester Institute of Technology, Rochester, New York, USA

An image quality investigation of visible spectral imaging systems was performed. Spectral images were simulated using different combinations of imaging system parameters with different numbers of imaging channels, wavelength steps, and noise levels based on two practical spectral imaging systems. A mean opinion score (MOS) was determined from a subjective visual assessment scale experiment for image quality of spectral images, rendered to a three-channel LCD display. A set of image distortion measures, including color difference for color images, were defined based on image quality concerns. The relationships between the distortion factors and the combinations of parameters in spectral imaging systems are discussed in detail. The MOS values and distortion measures were highly correlated. The results indicate that the image quality of spectral imaging systems was significantly affected by the number of channels used with noise in the image capture stage. The selection of wavelength steps had no significant impact on final image quality, especially when there was no noise involved. The results also showed that the contrast factor indicates a different impact on image quality for human portraits compared to other relatively complex scene images. An empirical metric is proposed to estimate the scaled image quality. The correlation between this metric and the subjective measure, MOS, was 0.97. The results also indicate that two distortion factor eigenvectors were sufficient to represent four distortion factors used in this experiment. This suggests that further research needs to be performed to find more efficient distortion factors.

Journal of Imaging Science and Technology 48: 211–221 (2004)

Introduction

As the applications of spectral imaging in the visible regime become increasingly popular,[1–4] image quality studies in this field have been of greater practical interest.[5,6] Most previous research in spectral imaging concentrated on the accuracy or optimization for color and spectral reproduction. However, little has been studied on the evaluation of overall quality of spectral images obtained by digital spectral imaging systems. Typically, when designing a wideband visible spectral imaging system, it is important to select the proper number of channels to capture the images. For instance, spectral imaging for art work may need more than six channels to accurately capture the spectral images while three channels are quite enough in spectral imaging for human portraits. During the processing stage, while applying principal component analysis (PCA) methods, it is important to select the proper number of basis functions and transform matrices to construct the spectral images. Mostly, however, those selections have been based only on the accuracy for color or spectral reproduction, not specifically for best image quality. Often, one needs to balance the accuracy of spectral information and noise tolerance of the spectral images. Based on PCA methods, more channels, or more basis functions, will give more accuracy of reconstructed spectral information. However, in most cases, more channels or more basis functions used will yield more noise in the reconstructed spectral images.[5]

Another issue is the wavelength increment used in representing spectra. Different spectral measuring instruments provide different levels of accuracy, such as 2 nm, 5 nm and 10 nm wavelength increments. Larger wavelength increments in spectra will require less image computation time and less space to store spectral images. There is little information about the impact of different wavelength increments on the image quality in spectral imaging. Other issues, like the stability of the transform matrix and the selection of objective function in imaging system optimization, will also impact the image quality of final spectral images.

To investigate those practical questions, image quality studies for spectral imaging are, therefore, worth pursuit. It was hoped that this image quality study could provide us a guide to improve our spectral imaging system for better quality of spectral images in future research. The present research does not try to solve all practical questions, but limits its goal to some specific issues. This research incorporates visual psychophysical experimental evaluation of image quality for spectral images rendered on a three-channel LCD screen. The spectral images were simulated using different noise levels, different eigenvectors (and channels) and wavelength steps in a spectral imaging system. To bridge the gap between the physical measures and subjective visual perceptions of image quality, effort has been made to build the image quality metrics. Four such image quality metrics have been applied in

Original manuscript received July 14, 2003

▲ IS&T Member

Color Plate 1 is printed in the color plates section of this issue, p. 235.

* qun_sun@yahoo.com, mdf@cis.rit.edu

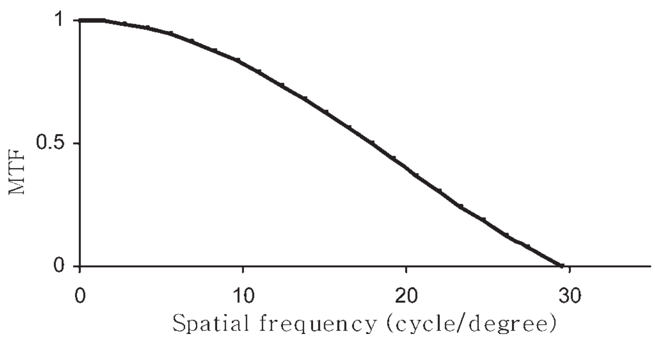

Figure 1. MTF of LCD display.

this research. The final goal is to find a single metric that is in good correlation with the subjective measure, MOS in this research.

Objective Distortion Factors

Four distortion factors were defined in this research. They are: color difference factor for color images; sharpness factor; graininess factor; and contrast factor.

Color Difference Factor

When dealing with reproduction of color imagery the color difference equation using s-CIELAB[7] is often selected to evaluate the color reproduction. In this research a procedure proposed by Johnson and Fairchild,[8] with a small modification of adding a modulation transfer function (MTF) of the LCD display to the luminance channel, was followed. The key of Johnson and Fairchild's method is to perform filtering in the frequency domain for opponent color signals in the traditional s-CIELAB method proposed by Zhang and Wandell.[7] The MTF of the LCD, as shown in Fig. 1, was derived based on Barten's[9] method with some practical modification. The mathematical expression of MTF is given in Eq. (1) where f is the angular frequency at the eye of the observer in cycle per degree (cpd) and k is the pixel distance of LCD display in visual angle.

$$MTF(f) = \left| \frac{\sin(1.2 \cdot k \cdot \pi \cdot f)}{1.2 \cdot k \cdot \pi \cdot f} \right| \tag{1}$$

Graininess Factor

Typically, root mean square (RMS) granularity is popularly used as an objective measure in evaluating the graininess of the images.[10] In this experiment, the objective measure of graininess was defined as the RMS error of original and its reproduction images, in the luminance channel of s-CIELAB opponent color space, after filtering as mentioned in previous section.

Sharpness Factor

To evaluate the effect of resolution on perceived image quality, Barten[11–13] proposed so-called square root integral (SQRI) as shown in Eq. (2).

$$SQRI = \frac{1}{\ln 2} \int_0^{f_{\max}} \sqrt{\frac{M(f)}{Mt(f)}} \frac{df}{f}, \tag{2}$$

where f is the angular spatial frequency at the eye of the observer in cycle/degree (cpd), f_{max} is the maximum angular spatial frequency displayed. $M(f)$ is the modulation threshold function (MTF) of the display, and $Mt(f)$ is the modulation threshold function of the eye. The inverse of the modulation threshold function of the eye is usually called the contrast sensitivity function (CSF) which is given in Ref. 13. Instead of using effective display luminance as in the Ref. 11, luminance values were calculated here using luminance factors given in Eq. (3).

$$L = 2 \cdot L_{LCD} \cdot Y/Ym, \tag{3}$$

where L_{LCD} is the luminance of LCD at white point, Y is mean Y tristimulus values of the image and Y_m is the Y tristimulus value of the LCD of the white point. It should be emphasize that SQRI is independent of image content. Researchers have indicated that SQRI values were correlated well to the subjective image sharpness for each individual image.[12–14] Its popular application and good performance in image sharpness analysis were the reasons it was selected as the sharpness factor in this research.

Contrast Factor

Calabria and Fairchild[15] proposed an empirical mathematical equation of Single Image Perceived (SIPk) contrast. This equation provides a tool to evaluate contrast in an image without reference to an original image. Though the validity of this equation for other image experiments requires further study, SIPk was selected as fourth distortion factor in this experiment. SIPk is given in Eq. (4).

$$SIPk = -1.505 + 0.131k_c + 0.151k_l + 666.216k_s, \tag{4}$$

where k_c, k_l, k_s are image chroma standard deviation, lightness standard deviation and the standard deviation of high frequency image lightness (filtering by Sobel filter) respectively. In this experiment, a factor of 10^{-3} was multiplied to the $SIPk$ as given in Eq. (4).

Visual Assessment Experiment

Spectral Imaging Simulation and Test Images

Four spectral images, fruit and painting,[16] and two human portraits[3] (one Caucasian, one Black) were used as original spectral imaging targets in simulation. Spectral images of fruit and painting were provided by researchers in Chiba University, and spectral images of human portraits were captured by authors using SONY DKC-ST5 digital camera. The details of spectral imaging for these four spectral images can be found in Refs. 3 and 16. The rendering images for these four spectral images are shown in **Color Plate 1, p. 235**, and were processed for display on a characterized LCD display in this experiment. Two imaging systems were simulated based on two real digital imaging systems. An IBM Research PRO/3000 Digital Camera System was used to simulate the spectral imaging for the fruit and painting targets. The SONY DKC-ST5 Digital Camera was used to simulate the spectral imaging for the human portraits. The spectral sensitivities of the digital cameras were measured directly using a calibrated measuring system consisting of spectroradiometer, illuminator and double monochromators. Details of spectral sensitivity measurement and digital camera settings can be found in Refs. 17 and 18. The spectral images of fruit and painting targets were simulated using three-channel, six-channel (by using 202 half C.T. blue filter, Professional Lighting Filters, Bogen) and nine-channel (by using 202 half C.T. blue filter and Kodak Wratten filter #66) wideband methods.[19] These filters were not optimized and were used only to avoid a big decrease for the blue channel signal. Mathematically, the application of these filters created additional independent equations for multi-band imaging. In simulation, these filters were used individually; they were not attached to each other during simulation for nine-channel wideband imaging. The spectral images of human portraits were simulated using three-channel and six-channel wideband methods (by using the 202 blue filter) while the original spectral images were obtained by using the six-channel wideband method with 2 nm wavelength steps.[3] The basis functions applied to fruit and painting targets were calculated from Vrhel's[20] data set including 170 natural and man-made object spectra, since those spectral samples are close to the spectra of fruit and painting. The basis functions used for human portraits were calculated from a previous spectral imaging experiment for human portraits,[12] since basis functions based on spectra of human portraits should provide the best color and spectral reproduction for spectral imaging of human portraits.

Five different wavelength steps were used to simulate the spectral image capture and reconstructing. They were 2 nm, 5 nm, 10 nm, 15 nm and 20 nm steps that are commonly used for commercial spectral measuring instruments. There are many distinct independent types of noise involved in digital imaging system. For simplicity in simulation and to limit the total number of target images for visual image quality assessment, simple uniformly distributed and channel independent random noise at 3 different levels was added into image capture stage in simulation. More practical and complex noise models are to be considered in future research. The noise levels were defined as zero noise, 1 percent noise, 2 percent noise and 3 percent noise (in terms of dynamic range of each channel). The random noise was channel independent and was created by pseudo-random variable generator using the IDL programming environment.[22] Therefore, including the originals, a total of 154 different spectral images were created, 46 for each fruit and painting target, and 31 for each portrait target. These spectral images were then converted into RGB images for LCD display. The illuminant D65 was used in spectral image processing for display.

Display Setup

The first step was to characterize the LCD. The details of the characterization technique were proposed by Fairchild and Wyble.[23] This research also performed optimization for LCD characterization that the black point of the LCD and the transformation matrix were optimized for best color accuracy. The accuracy of color difference in this experiment was 0.14 ΔE^*ab or 0.09 ΔE_{94} on average for 107 test data sets. In the next step, spectral images were converted into CIE 1931 XYZ images using illuminant D_{65}. The obtained XYZ images were then converted into XYZ images on LCD using chromatic adaptation.[24] Finally, XYZ images were converted to RGB values for LCD display using the LCD characterization.

The LCD display used in this experiment was a 22″ Apple Cinema Display. The resolution was 86 pixels per inch and the brightness was set to a peak luminance of 112 cd/m^2. The distance between the observers and the LCD was 60 cm. Therefore, the visual resolution was approximately 35.5 cycles per degree (cpd) as given in Eq. (5) where the d is the viewing distance in inches and ppi is the resolution. The image sizes displayed on LCD were 550 × 367 pixels for fruit and painting and 512 × 640 pixels for human portraits.

$$cpd = \frac{\pi}{180 \cdot \tan^{-1}\left(\frac{ppi}{d}\right)}. \tag{5}$$

Observers

A total of 32 observers, 18 experts and 14 novices, participated in this visual assessment experiment. Each image was compared to its original and repeated three times with random order displayed for the observers. The observers were asked to evaluate the image quality of reproduced images based on their corresponding original images. In other words, the observers were asked to evaluate the image quality based on the difference between a high quality image captured by a spectral imaging system and a "distorted" version of the same image. The following instructions were provided to the observers:

"This is an image quality visual experiment. We will display two images each time. The image on the left side is the original image, the image on the right side is the reproduction of the original or the original. Your task is to assign an image quality score to the right side image based on its overall image quality compared to its original on the left side. The quality score definitions are given as the following:
5: Excellent, no distortion is perceptible
4: Good, distortion is perceptible, but not annoying
3: Not good, not bad, slightly annoying
2: Poor, Annoying
1: Very poor, very annoying
0: Bad
You can also assign the score using steps of 0.5.
Thank you for your help and enjoy the experiment."

Experimental Results

MOS Values

As provided in Eq. (6), the observers were asked to assign an image quality score $A(i,k)$ to each image displayed on the right side on the LCD screen, where $A(i,k)$ was the score given by the ith observer to image k. For each reproduced image, the scores were averaged to obtain the MOS value for a specific image where n donates the number of observers.

$$MOS(k) = \frac{1}{n}\sum_{i=1}^{n} A(i,k) \tag{6}$$

To compare the differences of image quality scores obtained from expert and novice observers, the MOS from the novice observers versus MOS from the expert observers are plotted in Fig. 2. The correlation between MOS values from the expert and novice observers is 0.9961. The variation of image quality scores was estimated by the standard deviations of MOS values. The relationship between the standard deviations of MOS obtained from novice observers and the corresponding standard deviations of MOS obtained from expert observers is plotted in Fig. 3. The corresponding correlation is 0.9998. The mean standard deviation of MOS values obtained by experts is 0.57 while this value is 0.48 for novices. This indicates that the image quality scores assigned by the experts have more variation.

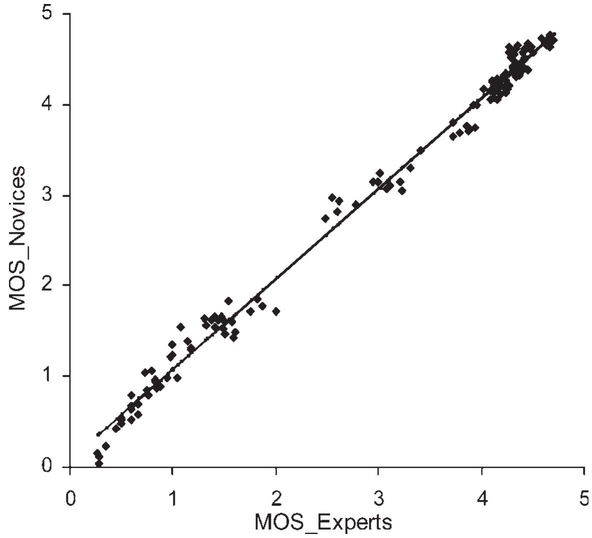

Figure 2. MOS from novice observers versus MOS from expert observers.

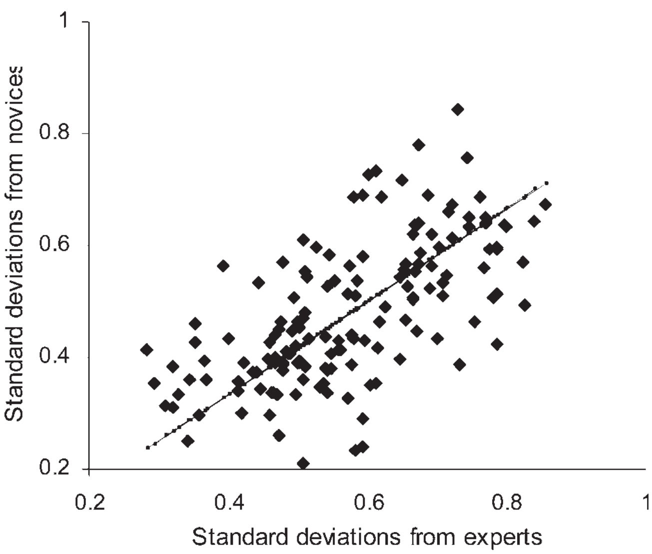

Figure 3. Standard deviations of MOS obtained from novice observers versus corresponding standard deviations of MOS obtained from expert observers.

Since the MOS values obtained from expert and novice observers are highly correlated, in the following they will not be discussed separately.

The MOS values for four image sets are shown in Fig. 4 where MOS values are plotted in terms of different number of basis functions. In Fig. 4, the notation Original represents the original images, 10 nm1N represents the reproduced images using 10 nm steps in wavelength and 1 percent noise under a certain number of basis functions. The rest of the notations follow similar definitions. Figure 4 indicates that image quality, as we expected, does relate to the number of channels or basis functions used in the imaging system when noise is involved. Considering Fig. 4(a), when using three basis functions, image quality was not significantly affected by the noise involved in the capture stage (within the noise range used in this experiment) for the relatively complex paint and fruit image sets. On the other hand,

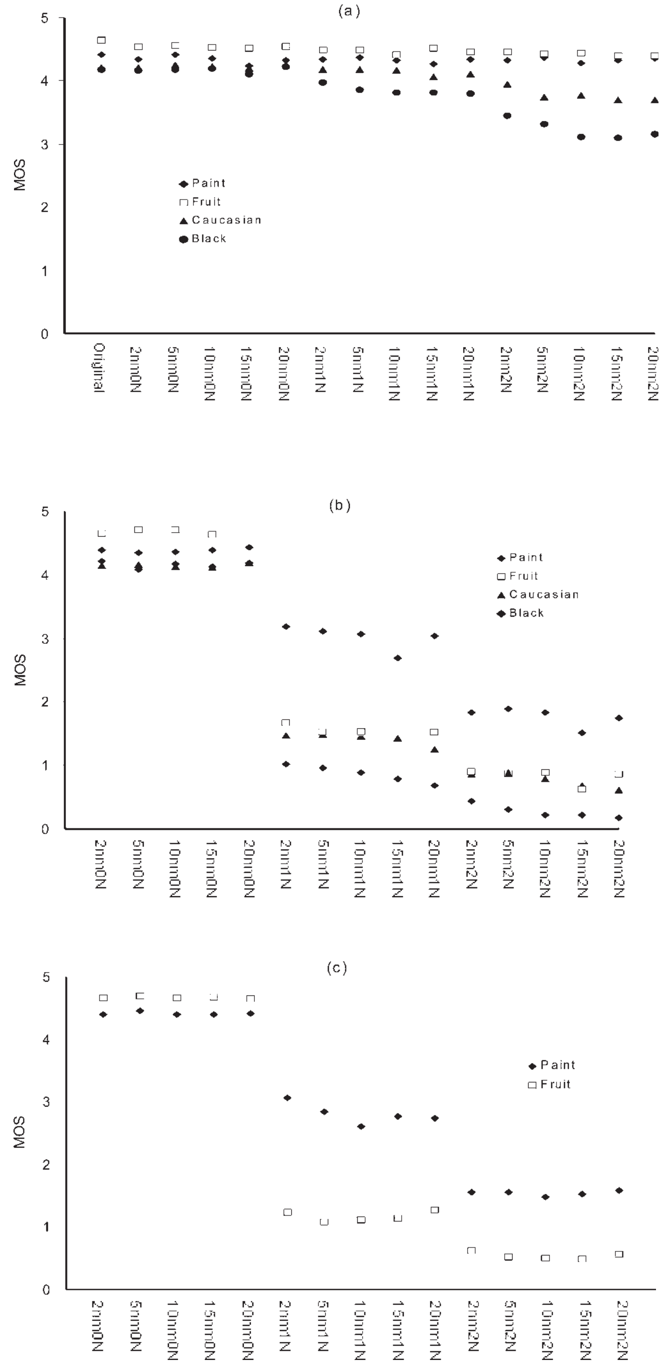

Figure 4. MOS values from image quality visual experiment. (a) Using 3 basis functions; (b) using 6 basis functions; (c) using 9 basis functions.

image quality was relatively more sensitive to noise for portrait image sets. This may be due to observers' greater ability to judge noise appearing on human faces compared to that of more complex images of painting and fruit. The human portrait images contain greater regions of low spatial frequency content. With the same noise levels, generally speaking, wavelength steps had no significant impact on image quality for all four image sets.

When using six basis functions as shown in Fig. 4(b), the image quality was impacted significantly by different noise levels; more noise provided lower image quality. Image quality of painting image sets was less sensitive to the noise compared to that for the other three image sets. This may be due to the fact that painting image sets contained relatively more high frequency information and could mask much of the noise effect compared to that of other three image sets. Generally speaking, with the same noise levels, the wavelength steps played no significant effect with respect to the image quality for all four image sets with the exception of using wavelength steps of 15 nm for painting and fruit image sets. The reason is unknown at this stage.

When using nine basis functions for painting and fruit image sets as shown in Fig. 4(c), the image quality effects were similar to those discussed for Fig. 4(b). Considering image quality using different number of basis functions, the image quality was impacted significantly; the more basis functions or channels used, the greater the noise effect shown and the poorer the image quality. This is consistent with the noise propagation theory in multispectral imaging systems proposed by Burns.[5]

Color Difference Factor Values

The color difference factor values for all image sets using different basis functions are plotted in Fig. 5; caution should be paid to the different scales used in Fig. 5. Figure 5 indicates that the color difference of all image sets was impacted significantly by noise; the more basis functions used and the more noise involved, the larger the color difference for the images. At the same noise levels, for painting and fruit image sets, the color difference was not significantly sensitive to different wavelength steps used with the one exception of using 15 nm steps while applying six basis functions. On the other hand, at the same noise levels, the color difference was significantly impacted by using different wavelength steps for portrait image sets; the larger the wavelength steps, the larger the image color difference. The reason is because it is more difficult for human observers to detect the color difference in relatively complex scene images, such as the painting, due to the noise masking effect of high frequency image content, than for the images of relatively lower frequency content, such as human portraits. This also suggests that to get the same image quality, a higher quality imaging system is required for human portraits than that for other relatively complex scenes.

Graininess Factor Values

The graininess factor values for all images sets, applying different basis functions, are calculated and plotted in Fig. 6. The situations are very similar to those of color difference factor values. The relationship between graininess factor and color difference factor is demonstrated in Fig. 7, and the correlation coefficient between graininess and color difference may be as high as 0.9027. Therefore, no further details will be discussed here.

Sharpness Factor Values

The sharpness factor values of all image sets are plotted in Fig. 8. Overall, different noise levels and wavelength steps did not significantly impact the sharpness factor of painting image sets. The sharpness factor was also not significantly impacted by different wavelength steps. As shown in Figs. 8(a) and 8(b), the sharpness factor was more sensitive to the noise for the black image sets. Figure 8 also indicates, more or less distinctly, that the sharpness factor of spectral images is more sensitive to noise when more basis functions are employed; the more basis functions employed and more noise (within the range of this experiment), the sharper of the images. This is a combined phenomenon previously reported by Sun and Fairchild,[3] and Johnson and Fairchild.[25] Sun and Fairchild reported that the spectral images were sharper when more basis functions were used, probably also due in part to greater noise. Johnson and Fairchild indicated that additive noise, up to a certain level, increased perceived sharpness.

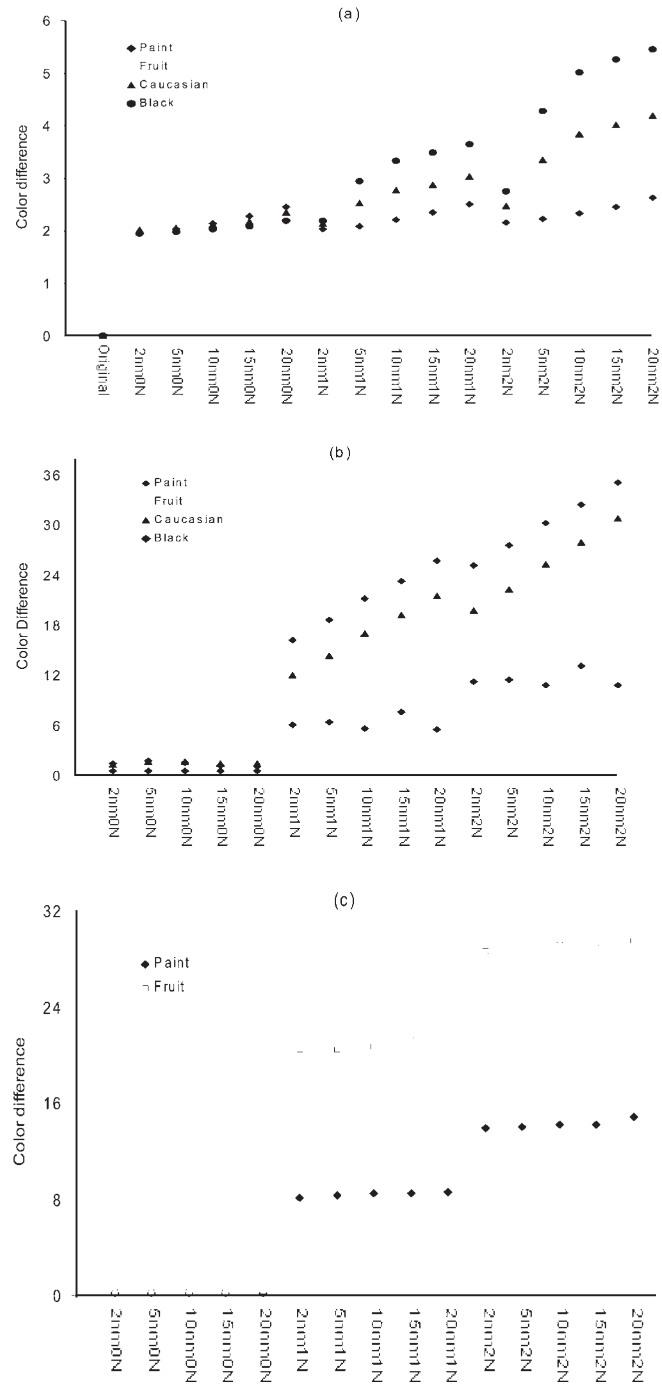

Figure 5. Color difference factor values from image quality visual experiment. (a) Using 3 basis functions; (b) using 6 basis functions; (c) using 9 basis functions.

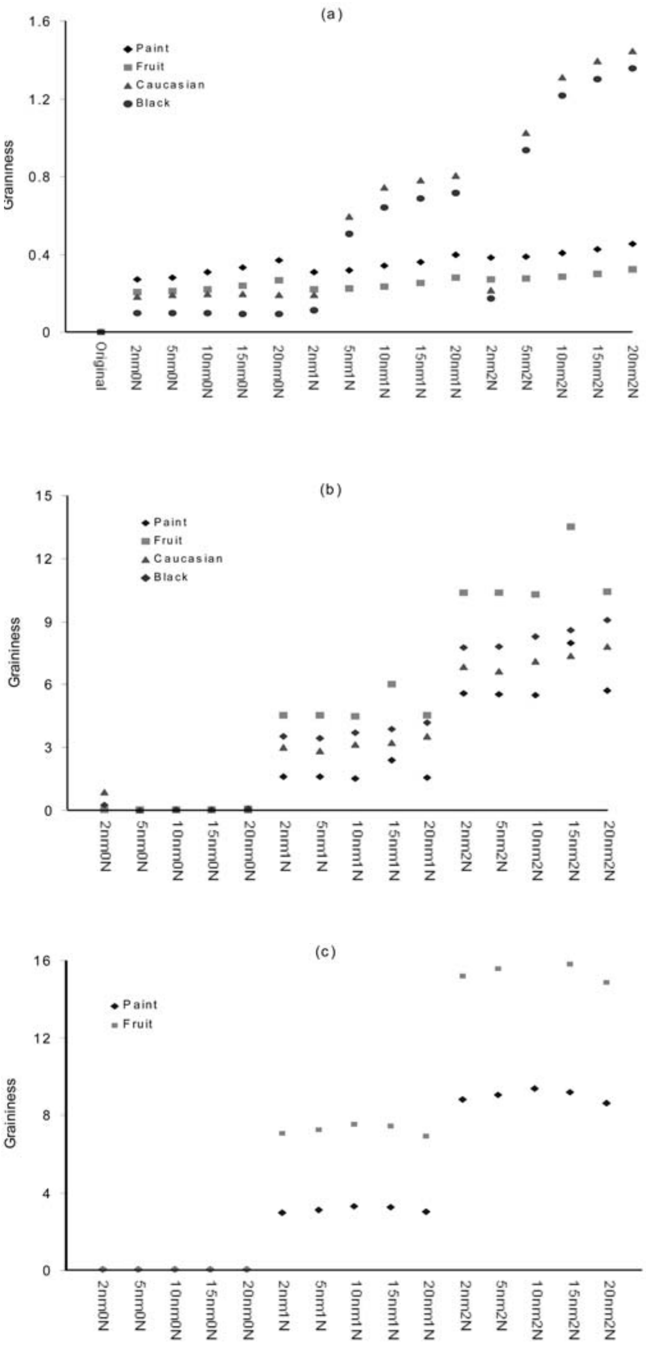

Figure 6. Graininess factor values from image quality visual experiment. (a) Using 3 basis functions; (b) using 6 basis functions; (c) using 9 basis functions.

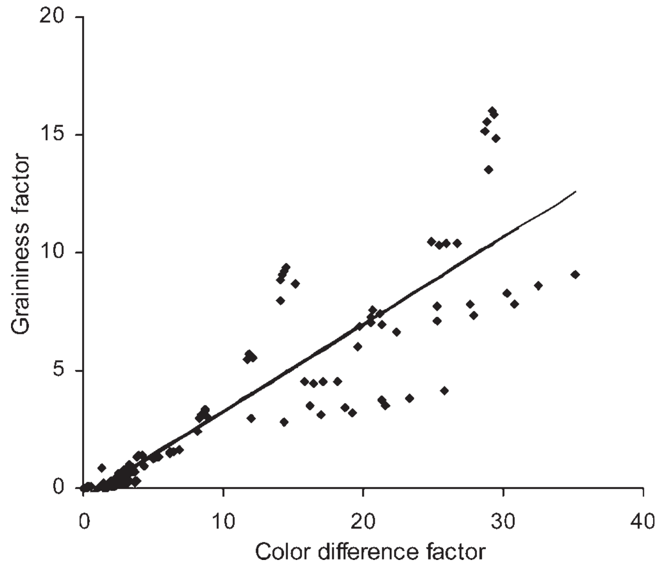

Figure 7. The relationship between graininess factor and color difference factor.

Contrast Factor Values

The contrast factor values of all image sets are plotted in Fig. 9. Contrast factor was not significantly impacted by different levels of additive noise and different wavelength steps when using three basis functions as shown in Fig. 9(a). However, the contrast factor showed three distinct groups when using six basis functions, as shown in Fig. 9(b). The contrast of portrait images increased with more additive noise. However, the contrast of paint images displayed just the opposite direction of portrait images. The contrast of fruit image sets, on the other hand, showed their own distinct characteristics. With one percent additive noise, the contrast of fruit images decreased. The contrast of fruit images would then increase when adding two percent noise. When using nine basis functions, as shown in Fig. 9(c), the contrast of paint and fruit images displayed the similar characteristics as in Fig. 9(b). Overall, the wavelength steps did not significantly impact contrast for all four image sets.

MOS Values versus Color Difference Factor

The relationship between the MOS values and their corresponding color difference factor values comparing the original images and their reproductions is shown in Fig. 10. The correlations between MOS values and color differences were 0.9876, 0.9865, 0.9706 and 0.9762 for Figs. 10(a) to 10(d) respectively. However, Fig. 10 indicates that the relationship between MOS values and color difference factor is image dependent, which means the same MOS values will have different color difference factor values for different images. This suggests that the image quality is not a single function of color difference, though color difference factor may predict image quality quite well. Figures 10(a) and 9(b) show that color differences in the fruit image sets were more noticeable than those in even more complex images of the painting. Similarly, the color differences for the two portrait image sets were also more noticeable. This might be due to the mechanism of frequency filtering in the human visual system. Figure 10 also indicates that larger color differences are proportional to the lower image qualities.

MOS values and their corresponding standard deviations of image color difference (compared to the original image) also correlated very well. They are plotted in Fig. 11 where the correlation coefficients are 0.984, 0.991, 0.993 and 0.990 for Figs. 11(a) to 11(d) respectively. Higher standard deviation of image color difference corresponds to lower image quality.

MOS versus Graininess Factor

Figure 12 shows the relationship between graininess factor and MOS value for painting, fruit, Caucasian and Black image sets respectively. MOS and graininess fac-

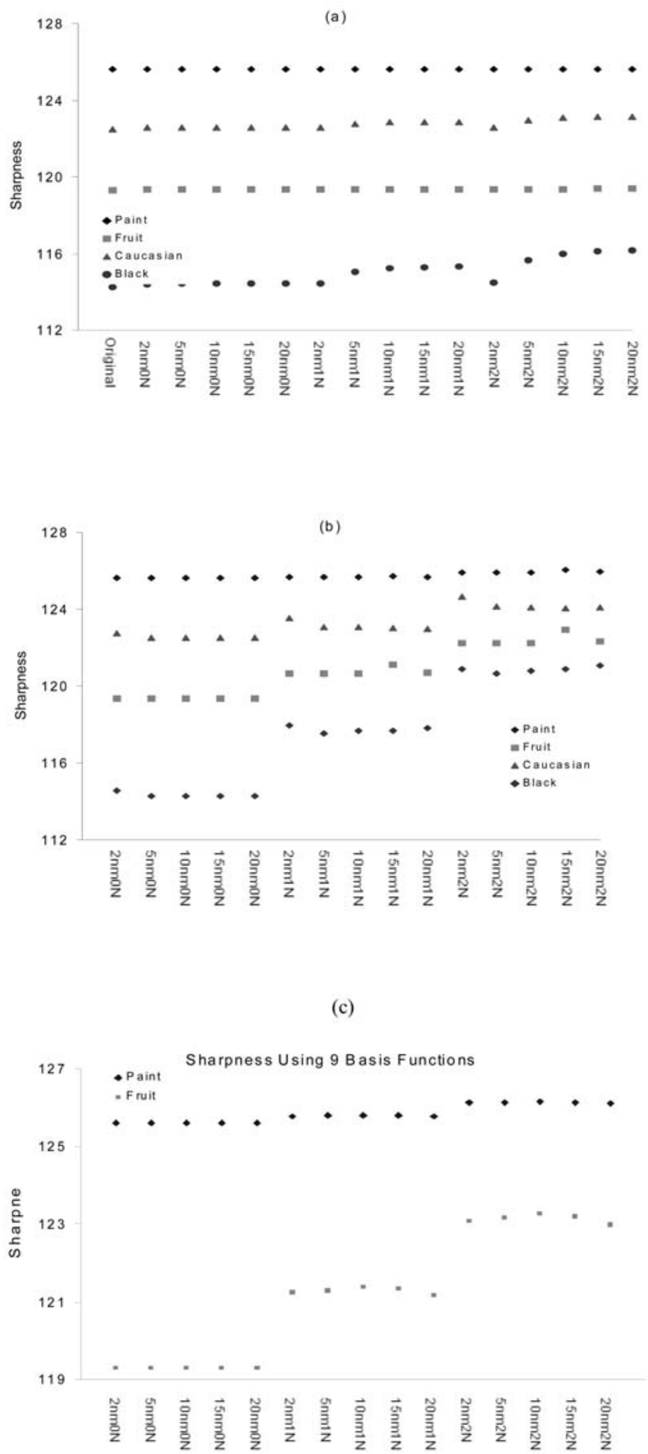

Figure 8. Sharpness factor values from image quality visual experiment. (a) Using 3 basis functions; (b) using 6 basis functions; (c) using 9 basis functions.

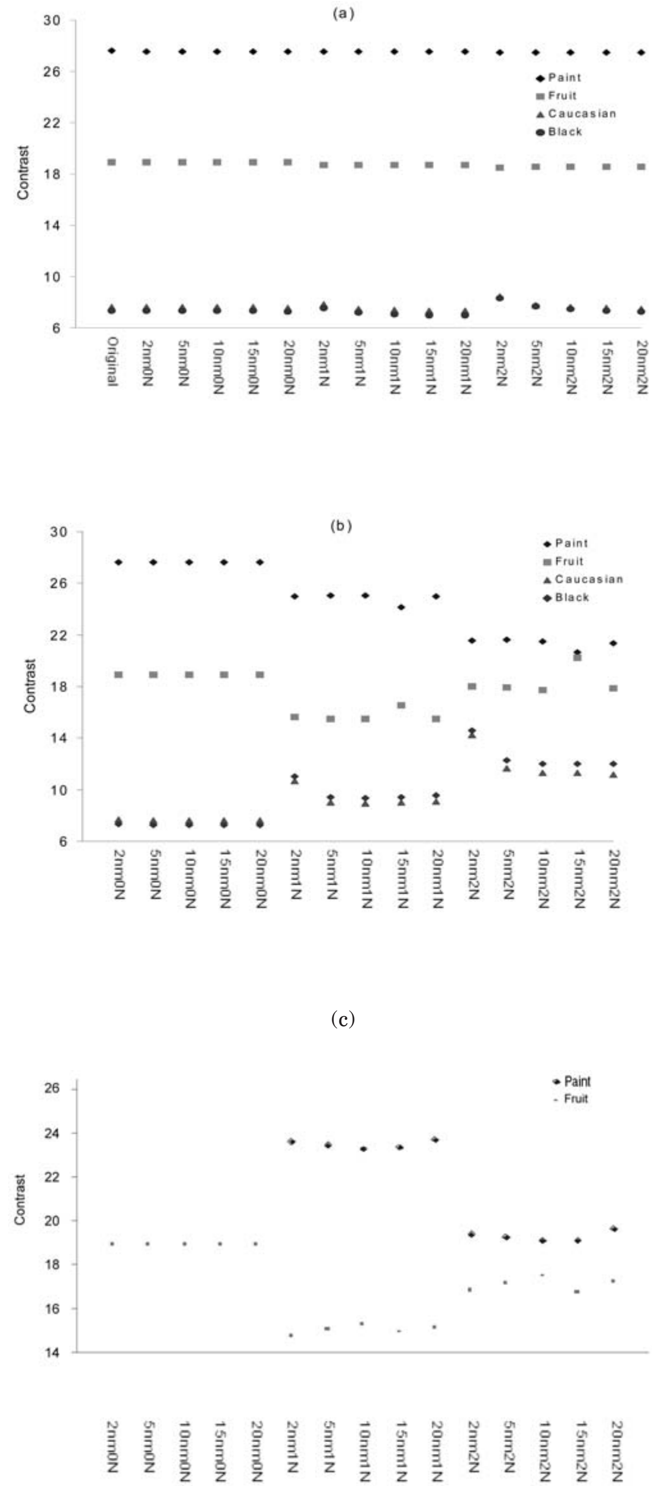

Figure 9. Contrast factor values from image quality visual experiment. (a) Using 3 basis functions; (b) using 6 basis functions; (c) using 9 basis functions.

tor correlated very well with the correlation coefficients of 0.95, 0.93, 0.93 and 0.93 for each image set, with high graininess value corresponding to low image quality.

MOS Values versus Sharpness Factor

The sharpness factor values were calculated using Eq. (2). The relationship between MOS value and sharpness factor is shown in Fig. 13. The sharpness factors correlated with MOS values very well with correlation coefficients of 0.946, 0.949, 0.850 and 0.952 for Fig. 13(a) to 13(d) respectively. Except for the Caucasian images set, MOS values correlated with sharpness factor values quite well. The reason this generalization does not extend to the Caucasian image set is unknown at this

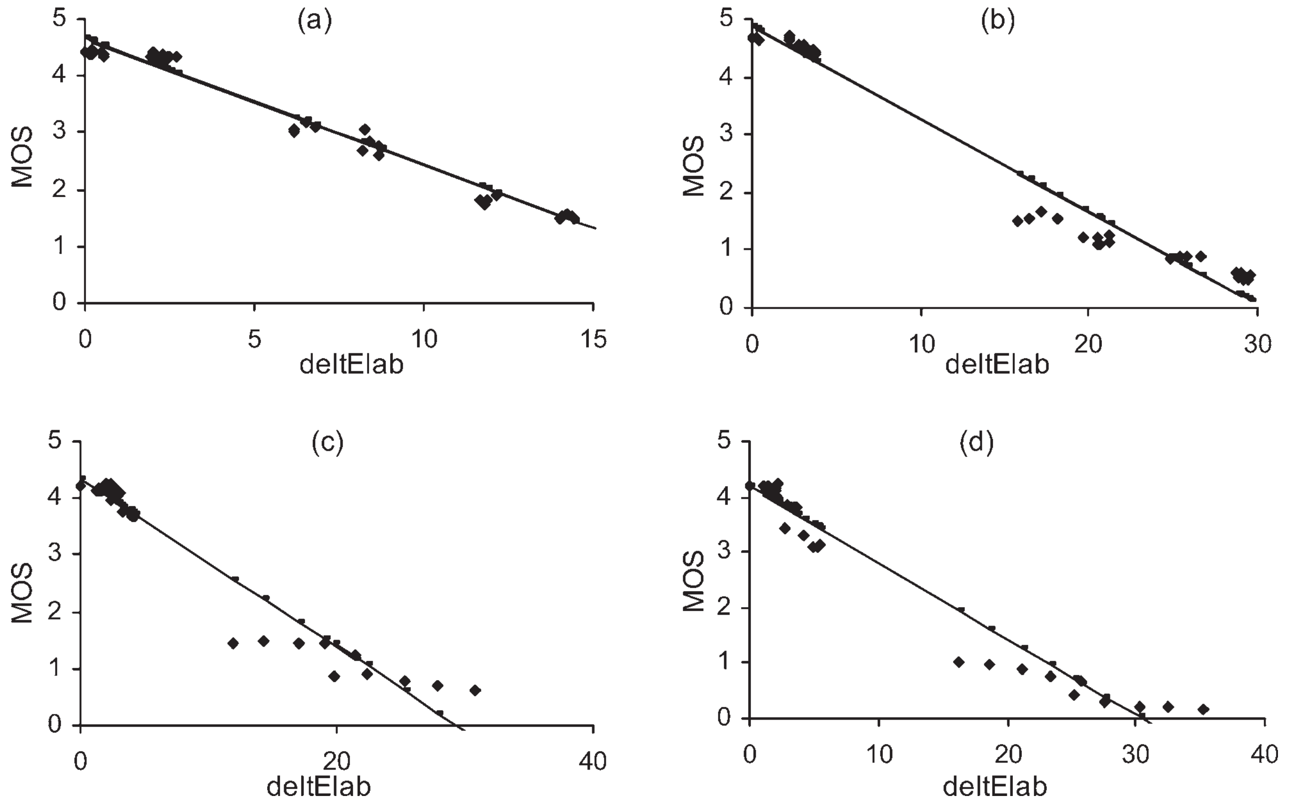

Figure 10. MOS versus image color difference factor. (a) painting images; (b) fruit images; (c) Caucasian images; (d) Black images.

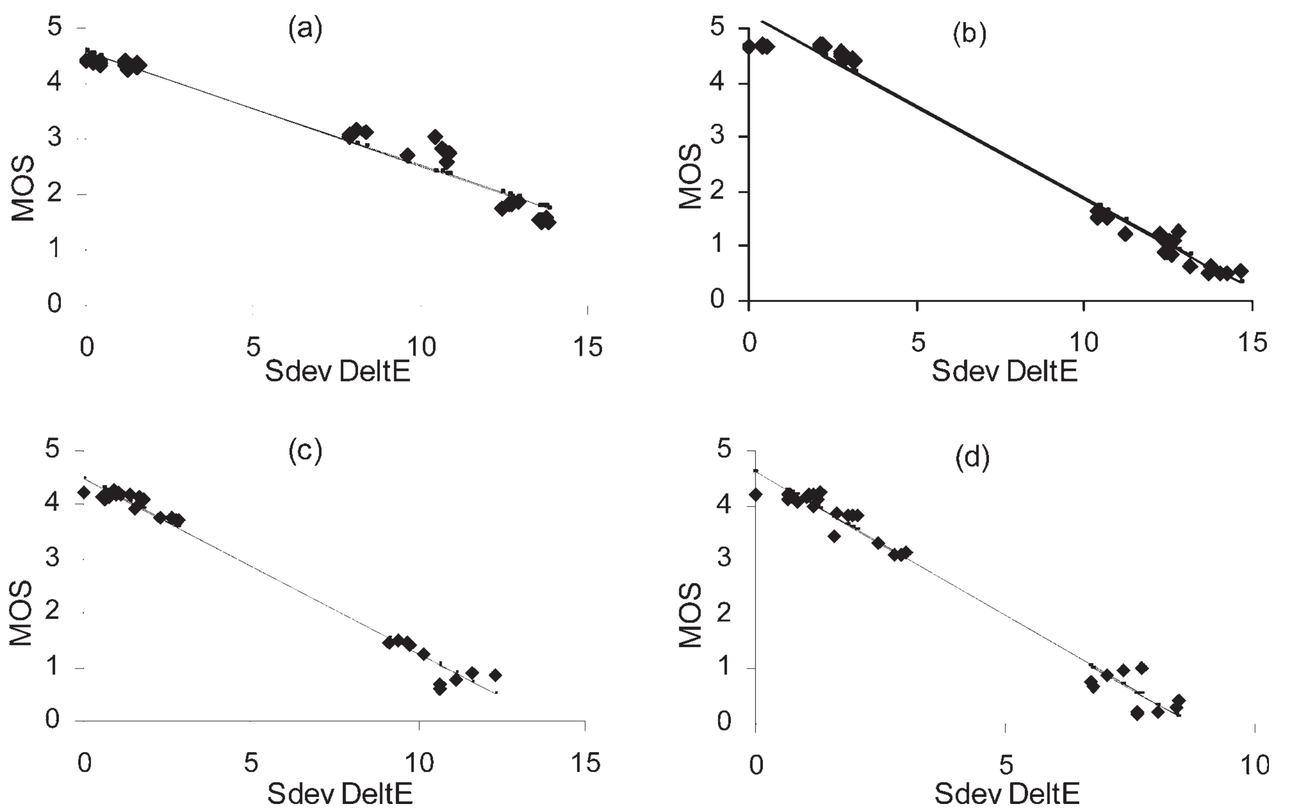

Figure 11. MOS versus standard deviation of image color difference factor. (a) painting images; (b) fruit images; (c) Caucasian images; (d) Black images.

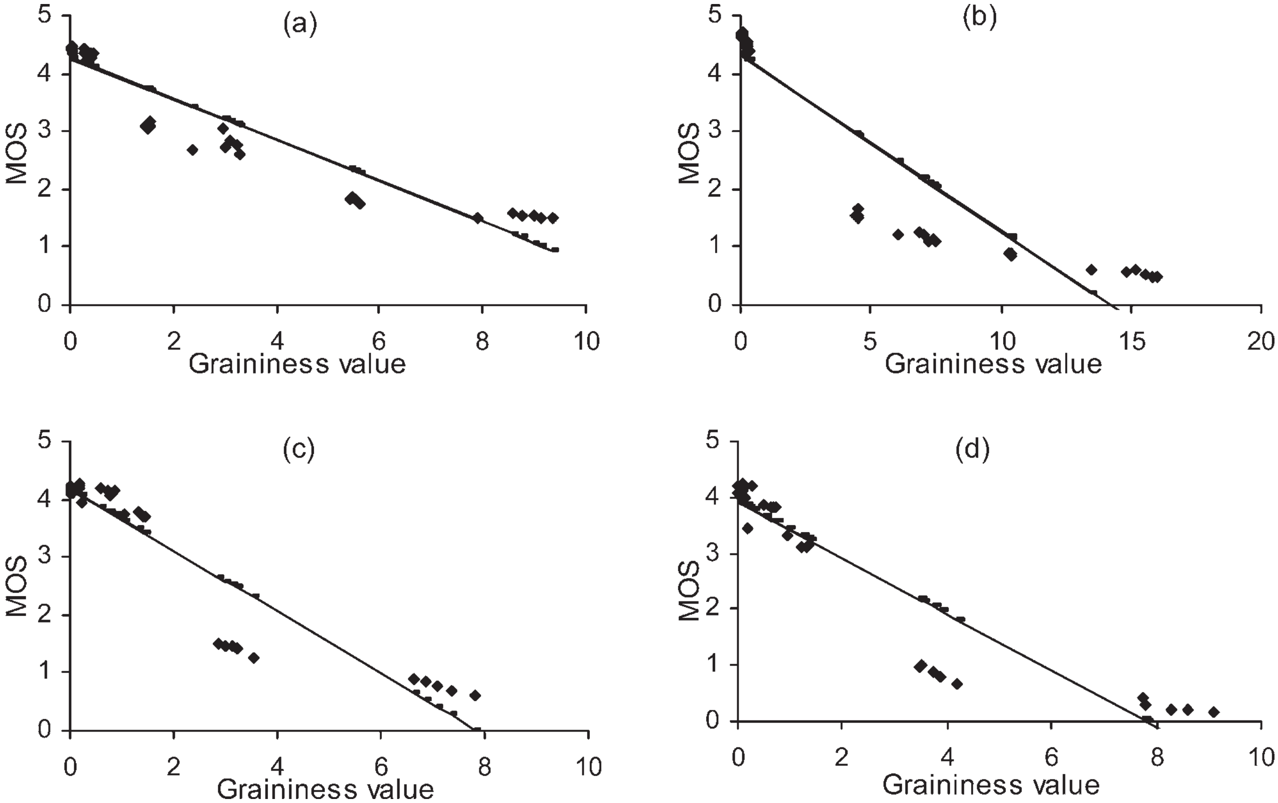

Figure 12. MOS versus graininess factor. (a) painting images; (b) fruit images; (c) Caucasian images; (d) Black images.

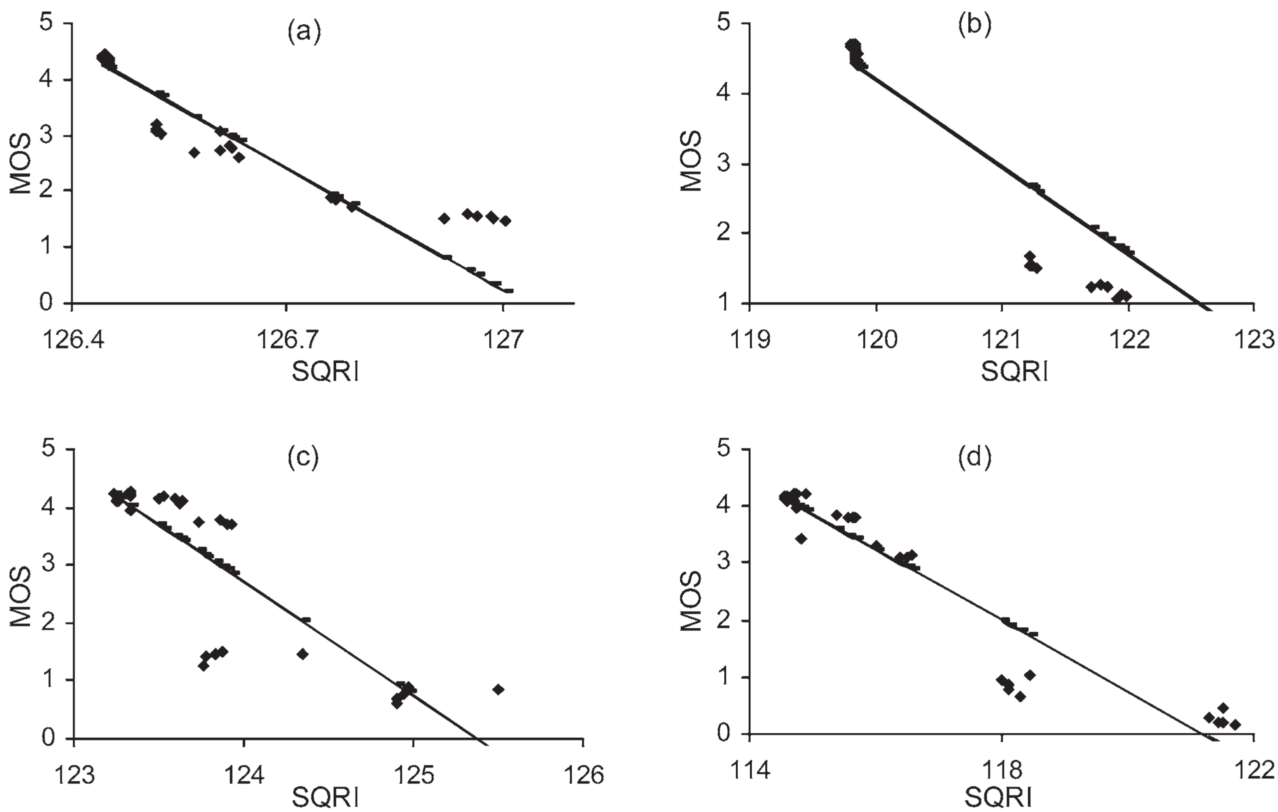

Figure 13. MOS versus sharpness factor. (a) painting images; (b) fruit images; (c) Caucasian images; (d) Black images.

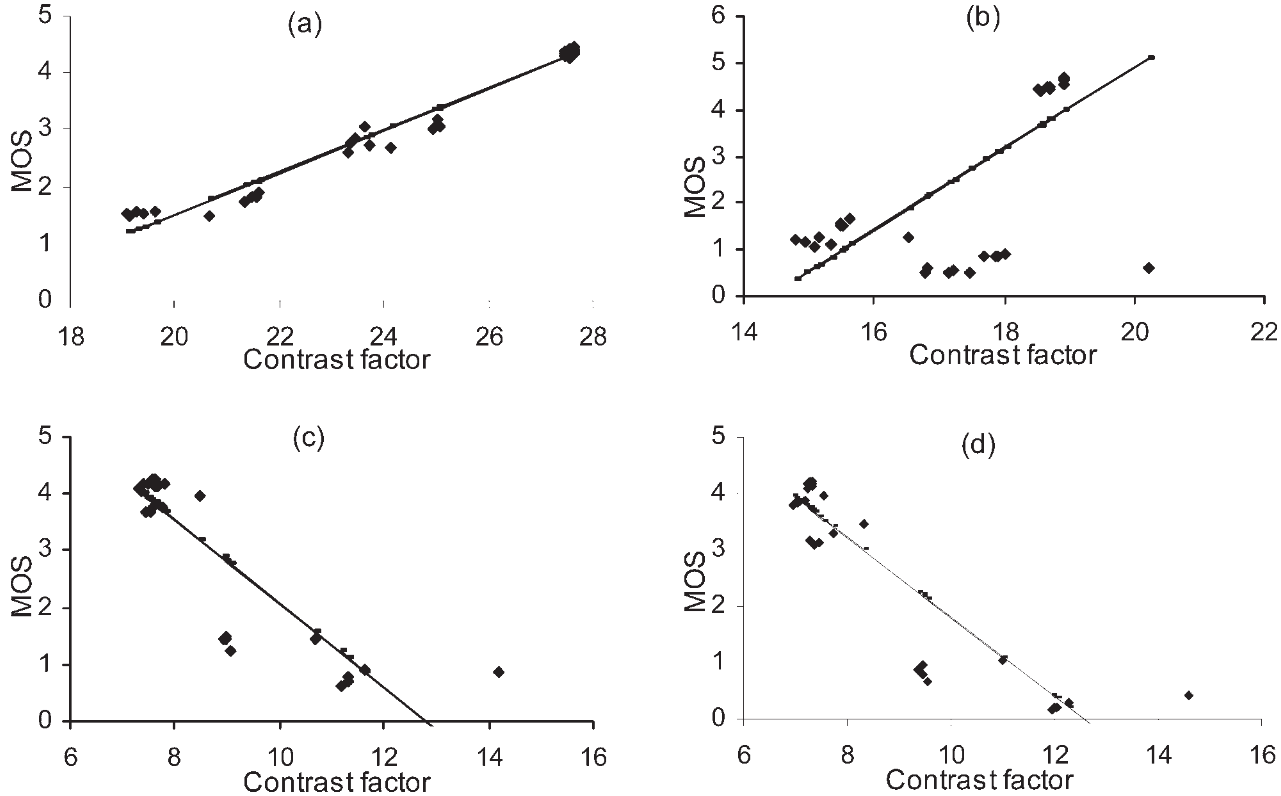

Figure 14. MOS versus graininess factor. (a) painting images; (b) fruit images; (c) Caucasian images; (d) Black images.

stage. Perhaps it is necessary to include other image parameters, such as color hue and gamma,[26] into Eq. (2) for better image quality prediction. Similar to the situation in Fig. 10, Fig. 13 indicates that the relationship between MOS values and sharpness factor values is image dependent, which means the same MOS values will have different sharpness factor values for different images. This suggests that image quality is also not a single function of sharpness factor. Figure 13(a) indicates that the sharpness factor values for painting images fell over a very small range compared to other image sets. Figure 13 also shows an interesting phenomenon that the larger sharpness factor values correspond to the lower image qualities in this research. This might also indicate that the original images were already sharp enough.

MOS versus Contrast Factor

The relationship between MOS and contrast factor values are shown in Fig. 14. The correlations between MOS values and contrast factor values are 0.988, 0.709, 0.873 and 0.901. Figures 14(a) and 14(b) indicate that these images with high contrast values displayed high quality. However, for human portraits, higher contrast factor values would display lower image quality. The reason is unknown and needs further investigation. Also, the correlations between MOS values and contrast factor values for fruit and Caucasian image sets were not high enough. Those are the issues need for future improvement and further investigation.

Empirical Quality Metric

A multiple regression analysis (MRA) was carried out between MOS values and distortion factors to determine

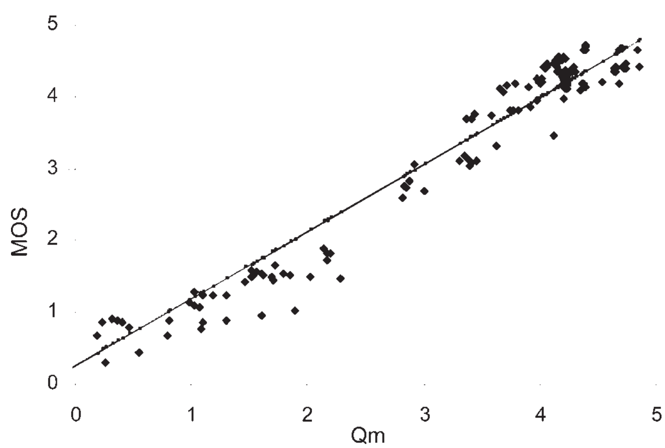

Figure 15. MOS versus Qm

one single image quality metric. The result is given in Eq. (7), where E is the color difference factor, G is graininess factor, S is sharpness factor, C is contrast factor and Qm is the quality metric. The correlation between MOS and Qm is 0.974. Figure 15 shows the relationship between MOS and Qm.

$$Qm = 6.07 - 0.1455E^{0.831} - 0.625G^{0.51} - 0.00387S^{1.305} + 0.254C^{0.351} \quad (7)$$

The distortion factors may be correlated since some of the image distortions contribute to several or all factors. A principal component analysis was performed to quantify the correlation between distortion factors. Results indicate that in this experiment, the first two eigenvectors will cover 98.9% and 99.9% of distortion factor variance respectively. Therefore, two eigenvectors are sufficient enough to represent these four distortion factors. This result may provide us with some direction to find more efficient distortion factors in future research.[27]

Conclusions

In this research, an image quality investigation in visible spectral imaging was performed. Spectral images were simulated using different numbers of imaging channels, wavelength steps, and noise levels, based on two practical spectral imaging systems. A mean opinion score (MOS) was determined from subjective visual assessment scale experiment for image quality of spectral images. A set of partial image distortion measures, color difference for color images, graininess, sharpness and contrast, were defined based on classified and quantified actual distortions produced by spectral imaging systems. When noise was involved in capture and reconstruction of spectral images, the number of channels or the number of basis functions selected had a significant effect on final image quality. With more basis functions employed, a higher noise effect is perceived. The wavelength steps did not have a significant effect on image quality, especially when no noise is involved. Apparently a wavelength increment of 10 nm is adequate for image quality in spectral imaging system. The results also indicate that a higher quality imaging system in terms of noise is required for spectral imaging of human portraits. The MOS and distortion measures were highly correlated, though further improvement in predictive modeling is a potential area for further research. The contrast factor shows opposite image quality effects on human portraits and other complex scene images in this experiment. The distortion factors defined in this experiment are highly correlated and need to be further investigated and refined.

Acknowledgment. The authors thank Dr. Francisco Imai for his spectral sensitivity data for the IBM digital camera, Dr. Garrett Johnson for his help and suggestions in programming, and researchers in Dr. Miyake's Lab, Chiba University, Japan, for their courtesy in providing spectral images of the painting and fruit. Eastman Kodak Co. provided financial support for the spectral portraiture imaging part of this research.

Reference

1. D. Tzeng, *Spectral-Based Color Separation Algorithm Development for Multiple-Ink Color Reproduction*, Ph.D. thesis, RIT, Rochester, NY, 1999.
2. R. S. Berns, F. H. Imai, P. D. Burns, and D. Tzeng, Multispectral-based Color Reproduction Research at the Munsell Color Science Laboratory, *Proc. SPIE* **3409,** 14–25 (1998).
3. Q. Sun and M. D. Fairchild, A New Procedure for Capturing Spectral Images of Human Portraiture, *Proc. SPIE* **4421,** 496–499 (2002).
4. S. Tominaga, Spectral Imaging by a Multi-Channel Camera, *IS&T/SPIE Conference on Color Imaging: Device-Independent Color, Color Hardcopy and Graphic Arts IV*, IS&T, Springfield, VA, 1999, pp. 38–47.
5. P. D. Burns, *Analysis of Image Noise in Multispectral Color Acquisition*, Ph.D. Thesis, RIT, Rochester, NY, 1997.
6. B. Hill, Optimization of Total Multispectral Imaging Systems: Best Spectral Match versus Lease Observer Metamerism, *Proc. SPIE* **4421,** 481–486 (2002).
7. X. M. Zhang and B. A. Wandell, A Spatial Extension to CIELAB for Digital Color Image Reproduction, *Soc. Inf. Disp. Sym. Tech. Digest* **27,** 731–734 (1996).
8. G. M. Johnson and M. D. Fairchild, A Top Down Description of S-CIELAB and CIEDE2000, *Color Res. Appl.*, in press (2003).
9. P. G. Barten, Resolution of Liquid-Crystal Display, *SID 91 Digest*, 772–775 (1991).
10. J. C. Dainty and R. Shaw, *Image Science*, Academic Press, Inc. New York, 1988.
11. P. J. Barten, The SQRI Method: A New Method for the Evaluation of Visible Resolution on a Display, *Proc. SID* **28,** 3, 253–261 (1987).
12. P. J. Barten, The Effects of Picture Size and Definition on Perceived Image Quality, *IEEE Trans. Elec. Dev.* **36,** 9, 1865–1869 (1989).
13. P. J. Barten, Evaluation of Subject Image Quality with Square-root Integral Method, *J. Opt. Soc. Amer. A* **7,** 10, 2025–2031 (1990).
14. S. Bouzit and L. MacDonald, Colour Difference Metrics and Image Sharpness, *Proc IS&T/SID 8th Color Imaging Conference*, IS&T, Springfield, VA, 2000, pp. 262–267.
15. A. J. Calabria and M. D. Fairchild, Compare and Contrast: Perceived Contrast of Color Images, *Proc IS&T/SID 10th Color Imaging Conference*, IS&T, Springfield, VA, 2001, pp. 17–22.
16. T. Fujimaki, K. Ishii, T. Ikeda, N. Tsumura, and Y. Miyake, Proposals of Standard Spectral Image and its Application to Designing of CCD Camera, *Proc. IS&T's 2003 PICS Conference*, 496–499 (2003).
17. F. H. Imai, Multispectral Image Acquisition and Spectral Reconstruction using a Trichromatic Digital Camera System Associated with Absorption Filters, *Munsell Color Science Laboratory Technical Report,* RIT, Rochester, NY, 1998.
18. Q. Sun and M. D. Fairchild, Spectral Image of Human Portrait, *Munsell Color Science Laboratory Technical Report*, RIT, Rochester, NY, 2000; http://www.cis.rit.edu/mcsl/online/Spectral/TechnicalPapers/SpectralImage_HumanPortrait.pdf.
19. F. H. Imai, Spectral reproduction from scene to hardcopy, Part I: Multispectral acquisition and spectral estimation using a Trichromatic Digital Camera System associated with absorption filters, *Munsell Color Science Laboratory Technical Report*, RIT, Rochester, NY, 2000; http://www.cis.rit.edu/mcsl/research/PDFs/Report.pdf.
20. M. J. Vrhel, R. Gershon and L. S. Iwan, Measurement and Analysis of Object Reflectance Spectra, *Color Res. Appl.* **19,** 4–9 (1994).
21. Q. Sun and M. D. Fairchild, Statistical Characterization of Face Spectral Reflectance and Its Application to Human Portraiture Spectral Estimation, *J. Imaging Sci. Technol.* **46,** 498–506 (2002).
22. http://www.rsinc.com/idl/
23. M. D. Fairchild and D. R. Wyble, Colorimetric Characterization of the Apple Studio Display (Flat Panel LCD), *Munsell Color Science Laboratory Technical Report*, RIT, Rochester, NY, 1998; http://www.cis.rit.edu/mcsl/research/PDFs/LCD.pdf.
24. M. D. Fairchild, Revision of CIECAM97s for Practical Application, *Color Res. Appl.* **26,** 418–427 (2001).
25. G. M. Johnson and M. D. Fairchild, Sharpness Rules, *Proc IS&T/SID 8th Color Imaging Conference*, IS&T, Springfield, VA, 2000, pp. 24–30.
26. P. G. J. Barten, Effect of Color Saturation and Hue on Image Quality, *Proc. IS&T's 2003 PICS Conference*, IS&T, Springfield, VA, 2003, pp. 16–21.
27. Q. Sun and M. D. Fairchild, Application of PQS for Image Quality Analysis in Visible Spectral Imaging, *Proc. IS&T/SID 11th Color Imaging Conference*, IS&T, Springfield, VA, 2003, pp. 132–136.

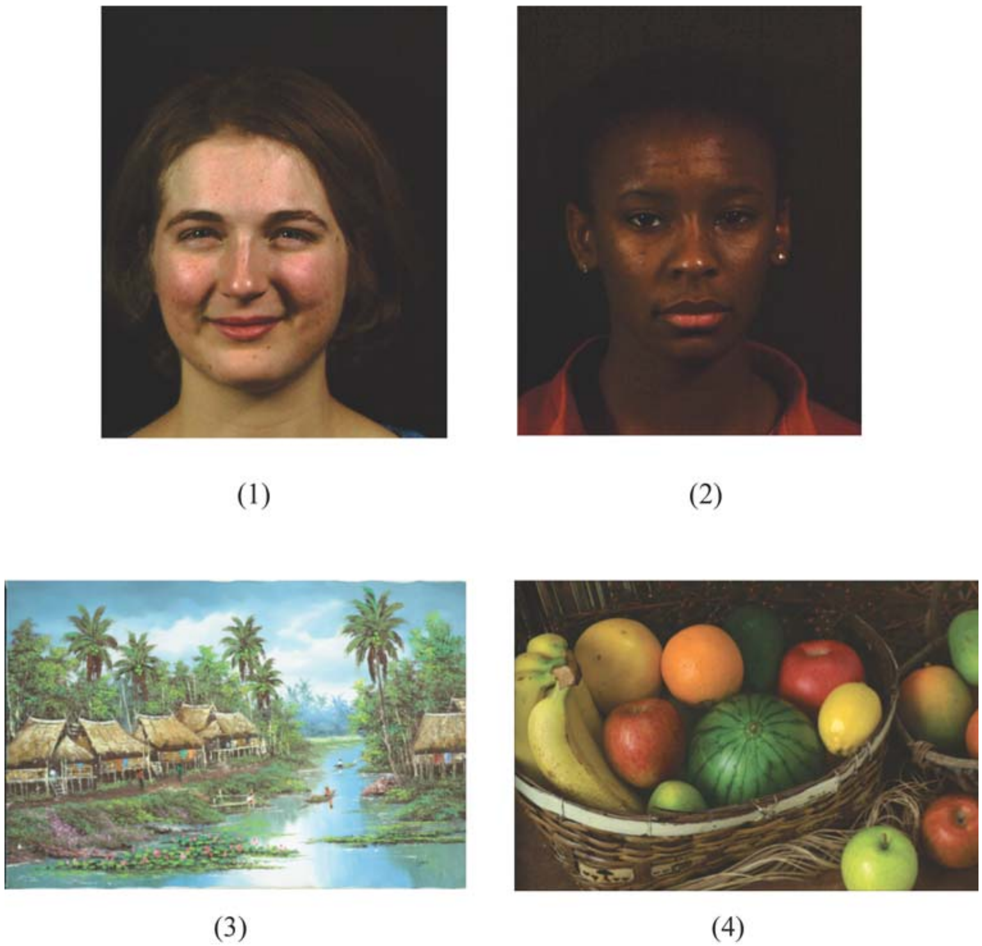

(1) (2) (3) (4)

Color Plate 1. Four spectral imaging objects for simulation. (1) Caucasian; (2) Black; (3) Painting; (4) Fruit. (*Sun and Fairchild,* pp. 211–221)